

## Hybrid Photo Detector Tests for the GlueX Project

V.D. Kovaltchouk, G.J. Lolos, Z. Papandreou, B. Ramadan, L. Snook, K. Wolbaum  
*SPARRO Group, Department of Physics, University of Regina, Regina, SK, S4S 0A2*  
July 4, 2002

### Abstract

The GlueX Experiment [1, 2] will employ a barrel calorimeter consisting of layers of scintillating fibers sandwiched between thin sheets of lead. Since this device will be positioned inside a 2 Tesla solenoid, its readout system must be able to function efficiently in this environment. The most promising candidate for a readout device is a hybrid photo detector (HPD). Tests of such a device from DEP Electronics (Model PP0350G) as well as of its associated pre-amplifier circuit are reported here.

### 1 Introduction

The barrel calorimeter (BCAL) is a crucial GlueX detector subsystem. This device will be responsible for the detection, identification and total energy measurement of all neutral (photons, neutrons) and charged (protons, pions and kaons) particles within its volume, ranging from 20 MeV to 1 GeV in energy. These requirements are coupled to the minimum inner radius of the BCAL, which will allow for the placement of the interior subsystems (chambers, start/vertex counter and target), and to set the maximum radial dimensions of the BCAL. Its longitudinal dimension is largely dictated by the length of the solenoid magnet, resulting in a nominal length of 4.5 m.

The BCAL will be read out at both ends, and the readout zone will be immersed in a high field (up to 2 Tesla) that also has a rapidly changing field gradient in space. Therefore, it is crucial to use a readout device that can operate at such field values. The only device in the market to date is based on a hybrid photo-multiplier design, which combines a photo-cathode with a PIN diode.

## 2 Hybrid Photo Detectors

### 2.1 Description

The DEP<sup>1</sup> HPD combines state-of-the-art solid state technology and the latest vacuum photo-cathode technology. These devices resemble conventional photo-multipliers (PMTs) in their operation, but their unique design makes them suitable for high magnetic field operations and provides for a good energy resolution.

Specifically, in our tests we used the DEP PP0350G HPD, coupled to a PP0100Z HV power supply, provided also by DEP (see Figure 1). This HPD is a proximity focused device that has a photo-cathode (S20-UV on fused silica) and PIN diode with an identical sized active area, separated by a small gap, as shown in Figure 2. The proximity of the photo-cathode and diode results in short electron trajectories, which, coupled with the use of non-magnetic materials in the vacuum pot of the HPD, renders the device immune to magnetic fields up to 2 Tesla, as shown in Figure 3. The spectral sensitivity of this device is shown in Figure 4.



Figure 1: *The PP0350G HPD (right) showing its overall size as well as its active area (innermost circle – photo-cathode window). Also displayed are the PP0100Z HV power supply (black box) and its custom-built voltage distributor (gray box).*

The HPD is powered by a HV supply which is typically set to -8 to -9 kV, and a bias of -60 to -80 V is applied across the diode. The gain response of the HPD as a function of

---

<sup>1</sup>Delft Electronic Products B.V., P.O. Box 60, 9300 AB Roden, The Netherlands

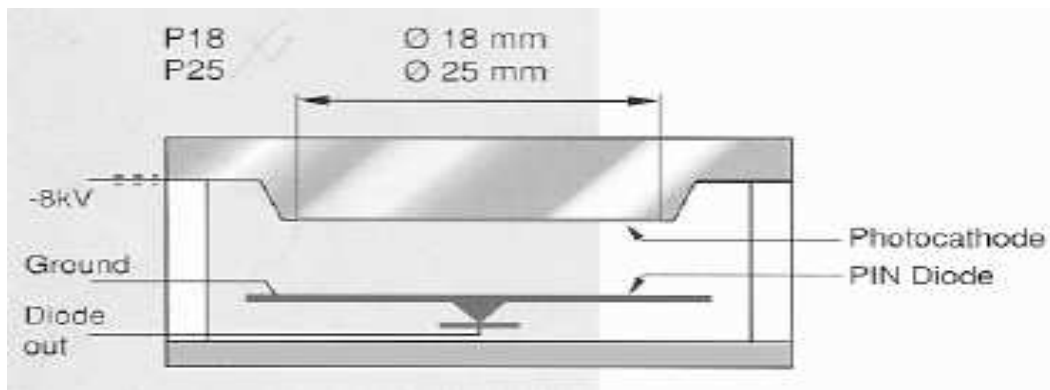


Figure 2: Schematic side view of the PP0350G HPD.

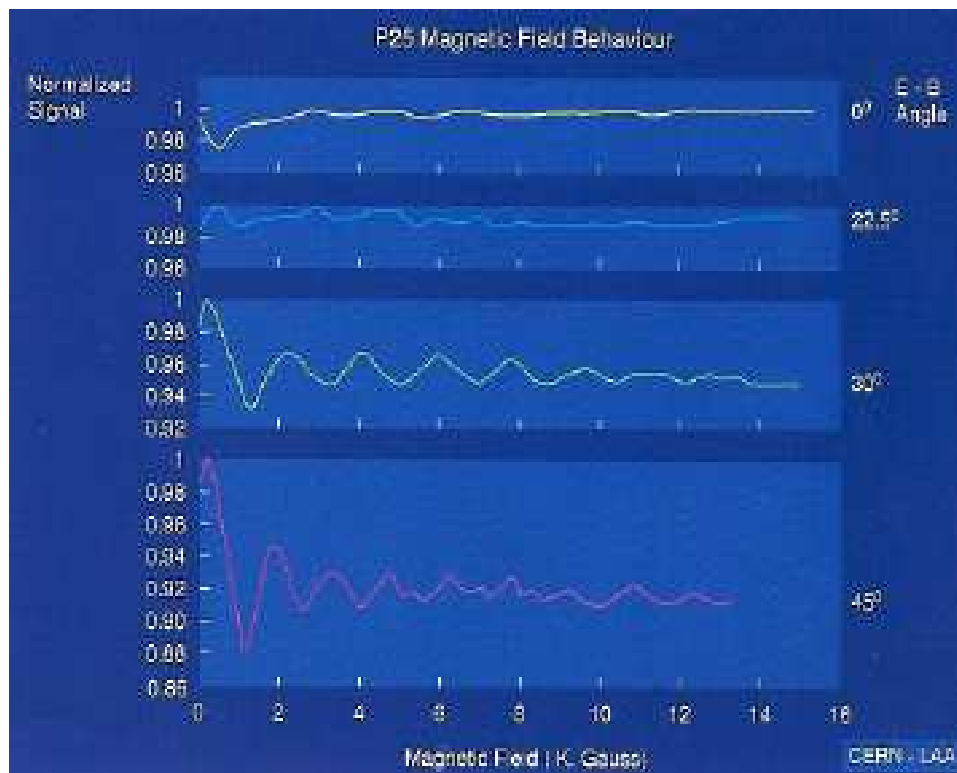


Figure 3: Magnetic field behaviour of the PP0350G HPD, for four different angles of the HPDs electric field with respect to the external magnetic field. Even when the angle is 45° the performance is not degraded severely.

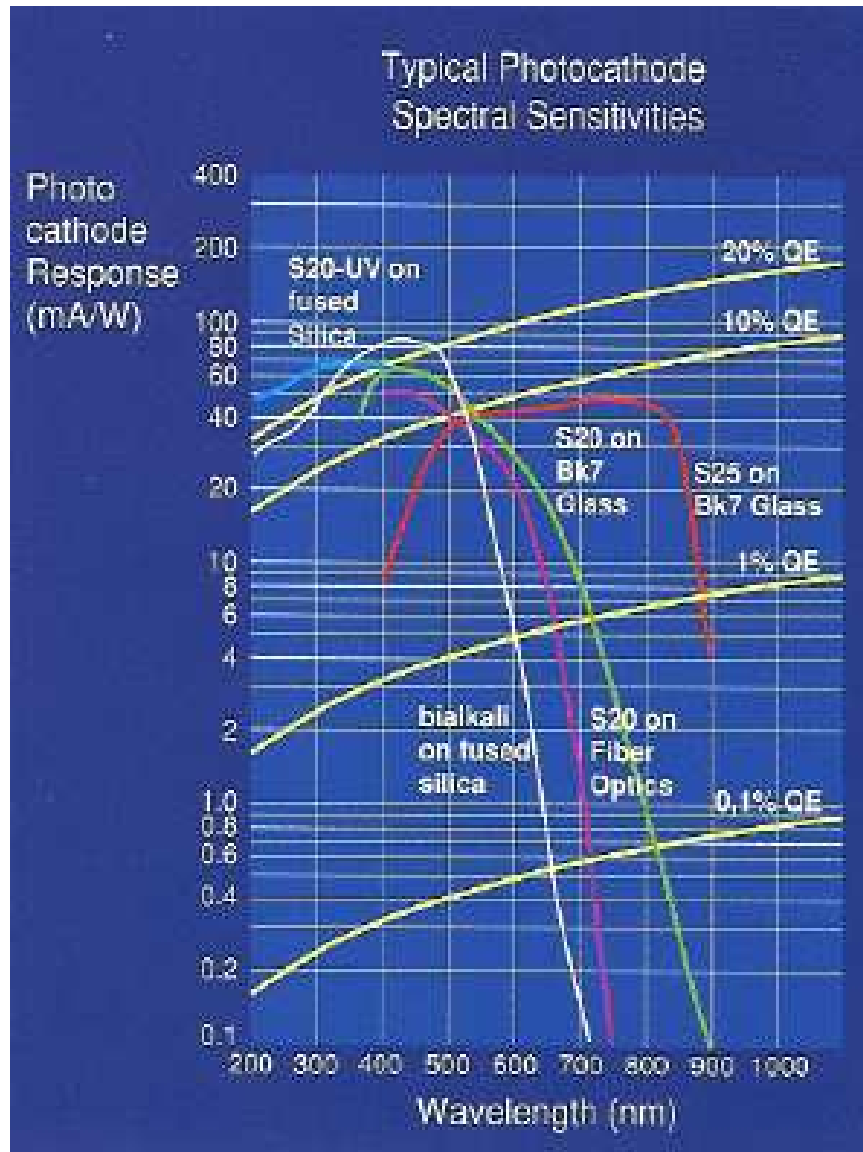


Figure 4: Spectral sensitivity: the PP0350G curve starts off as blue and continues as green around 380 nm. This device is ideally suited to receive light from scintillating fibers, whose light peaks at 430-450 nm and ranges from 380-550 nm.

HV and photo-cathode position is shown in Figure 5.

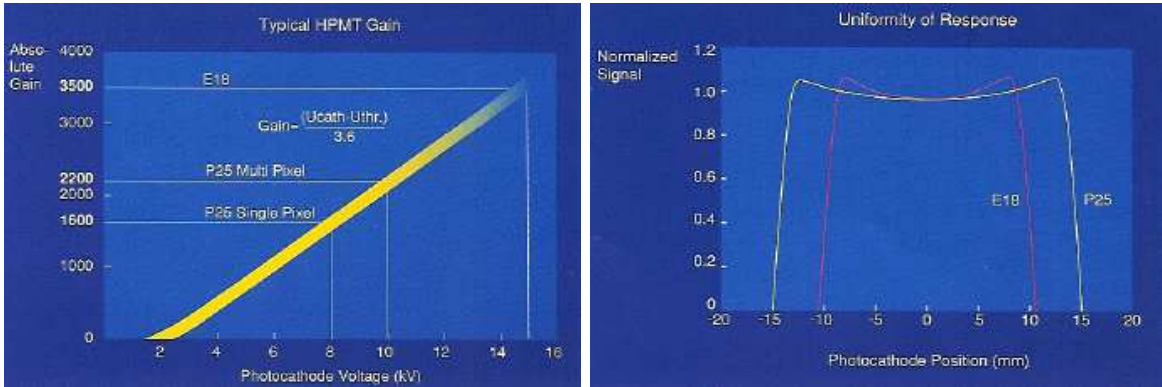


Figure 5: **Left panel:** Gain of the PP0350G (P25 single-pixel). **Right panel:** Uniformity as a function of photo-cathode position for the PP0350G (P25).

## 2.2 Electronic Circuit

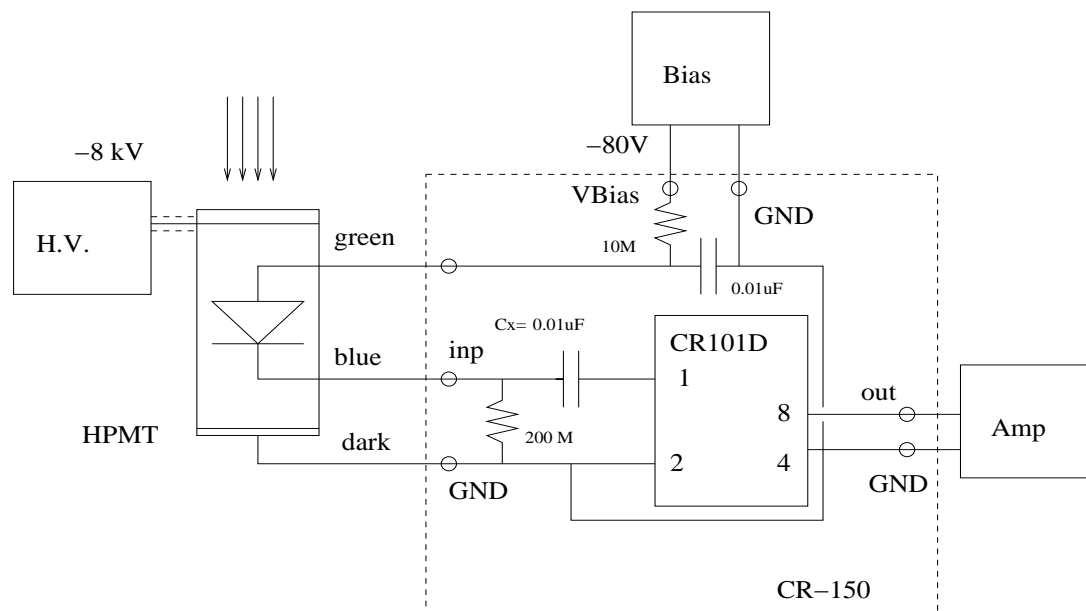
The PP0350G HPD has a gain of about 1600, which is insufficient for operational use with the relatively low-light situation of the optical fiber readout of the BCAL. The first step toward operational status was to design and construct an electronic circuit that would couple to the HPDs signal wires and whose main component would be a pre-amplifier chip. This chip should have a small rise time and should be reasonably priced, keeping in mind that 600 such circuits will have to be built for the full sized BCAL.

The chip that fulfilled these criteria was the Cremat<sup>2</sup> CR-101D charge sensitive pre-amplifier. Its rise time is 13 ns, its input capacitance is 20 pF and its power dissipation is 150 mW, the latter being another concern for the full sized BCAL. Finally, its price is quite reasonable: US\$45. The CR-101D was connected to the PP0350G as shown schematically (top) and pictorially (bottom) in Figure 6.

In all the work presented below, extreme care had to be exercised so as to electrically isolate the circuits. Much effort was expended in two main areas: a) the avoidance of current (ground) loops in the circuit and b) the shielding of the circuits from RF noise.

As far as ground loops went, carefully planned connections between the HPD, its power source, the pre-amp and the measuring instruments (e.g. oscilloscope) had to be exercised. In

<sup>2</sup>Cremat Inc., 45 Union Street, Watertown, MA 02472, USA.



PP0350G connection diagram

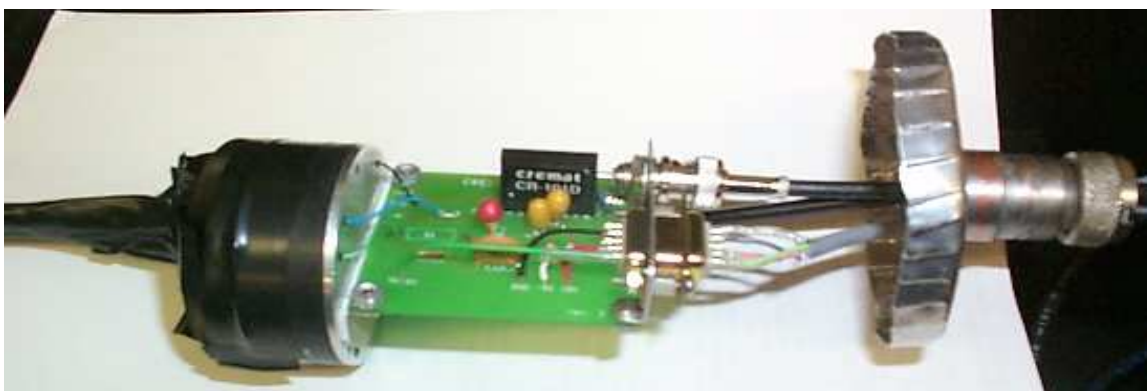


Figure 6: **Top panel:** PP0350G connection diagram. The main elements of the charge sensitive pre-amplifier Cremat CR-101D are indicated inside dashed box. The power supply (+/- 9V) is not shown in this figure. CR-150 is the circuit board on which the CR-101D pre-amplifier is mounted. **Bottom panel:** Image of the physical connection between the PP0350G (wrapped in black optical tape) and the electronics board. The Cremat CR-101D chip is clearly visible on the board.

the end, when very fine features (small amplitude) of the HPD signals were being examined, an uninterruptable power supply (UPS) and a custom-built battery pack were both used. These provided the maximum protection from ground loop effects.

The PP0350G is an extremely sensitive RF antenna. It is next to impossible to operate this device without a housing to shield it from the ambient RF noise. The constructed housing was composed of two parts: the inner and outer housing. The former (see Figure 7) served as a mount for the HPD and protected it from physical damage during the tests. At the HPD-window end, it was equipped with a collar design, to facilitate the coupling of light guides to the HPD. At the back end the HPD HV, signal and ground wires were soldered to the appropriate connectors that were mounted on a thin circular aluminum plate. This plate was coupled to the inner housing (see Figure 7) with a spring-loaded system. On the other hand, the outer housing was a simple copper jacket with an end cap to provide the main RF protection to the HPD.

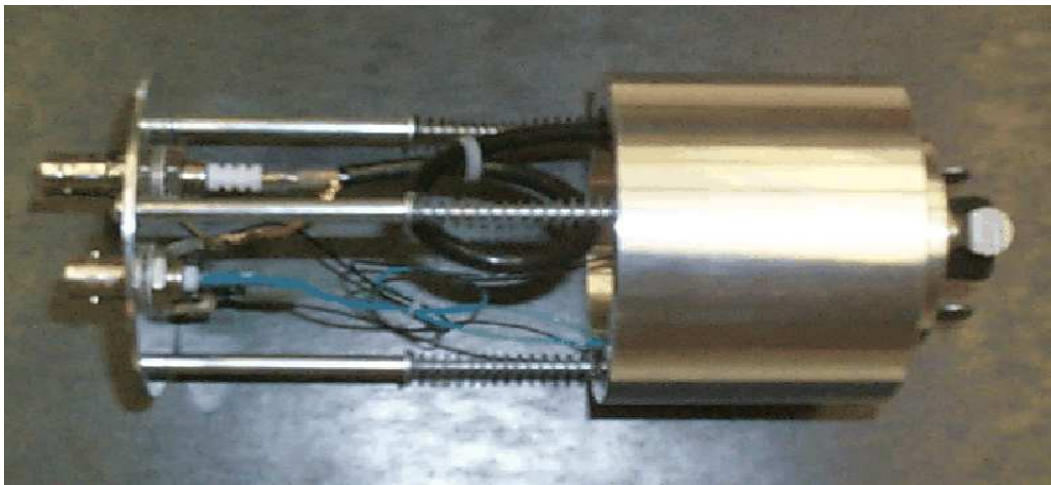


Figure 7: *The inner HPD housing.*

## 2.3 Measurements and Results

Several sets of measurements were carried out in order to investigate the performance of the HPDs, each set having a separate aim as listed below. The particulars and results of each set are presented in distinct subsections.

1. Study of rise time and amplitude of HPD signals.



Figure 8: *The outer HPD housing.*

2. Investigation of the spectroscopic response (energy spectrum).
3. Amplitude vs. gain relationship.
4. ADC Peak position as a function of diode bias voltage.
5. Low light level measurements (few photo-electrons).
6. Photo-cathode positional sensitivity.

### **2.3.1 Rise Time and Amplitude**

The setup for the measurement of the rise time and amplitude of the HPD is displayed in Figure 9. The results of the measurements are presented in Table 1 and Table 2. Both rise time and amplitude are strongly dependent on the effective capacitance ( $C_{eff}$ ) of the HPD plus pre-amp circuit. A decrease in  $C_{eff}$  results in a dramatic improvement in the rise time, typically from  $\approx 150$  ns to as low as  $\approx 30$  ns, at the expense of the amplitude, which drops accordingly from a signal to noise ratio of 20 to that of 4-5. Clearly, there is a trade-off in optimizing both parameters. This optimization will be determined in the future, once Monte Carlo simulations and detailed electronics information from other detector components of the GlueX experiment become available.



Table 1: **Rise time and signal amplitude behaviour**

Type	LS+10%		LS		Am+NaI		NaI+Cs	
	T	A	T	A	T	A	T	A
HPD		noise	22	10 mV				
HPD+50	<10	4.5 mV	<10	55 mV		2 mV		
HPD+100	<10	5.5 mV	<10	80 mV				
HPD*	150	1.4 V				2 V		
HPD*+50						1 V		
HPD*+100						1.5 V		800 mV
PMT	<10	8 V			350	35 V	350	17.5 V
PMT+50	<10	3 V			<10	2 V	<10	0.8 V
PMT+100	<10	4.3 V						

Notes are itemized below

- **LS:** Nanosecond Broad-Spectrum Optical Pulse Radiator (Model NR-1A) and Laser Pulse Simulator (Model LPS-1A). High Voltage: 20 kV.
- **LS+10%:** LS with 10% filter (neutral density) was used.
- **HPD:** A 25 mm proximity focused single pixel Hybrid Photo Diode equipped with an S20UV photo-cathode on a quartz input window. High Voltage: -8 kV, Bias: -75 V. PIN (Si) Diode capacitance: 200 pF. (See electronic setup in additional Figure 9).
- **HPD\*:** HPD with charge sensitive pre-amplifier CREMAT CR-101D. C=10000 pF input capacitance was used.
- **PMT:** Model: BURLE 8575. Serial number: N27671. High Voltage: -2 kV.
- **PMT+50:** PMT with shunting 50 Ohm resistance was used.
- **PMT+100:** PMT with shunting 100 Ohm resistance was used.
- **Am+NaI:** NaI(Tl) scintillator ( $\varnothing$ 6 mm and depth of 10 mm) with incorporated alpha source (Am-241, E=5.5 MeV). **NaI+Cs:** NaI(Tl) scintillator ( $\varnothing$ 12 mm and depth of 30 mm; Serial number: P260R; Type: 4D4P6) was irradiated by 662 keV gamma rays from Cs-137 ionization source.
- **T:** Rise time measured between 10% and 90% height of signal amplitude, in ns.

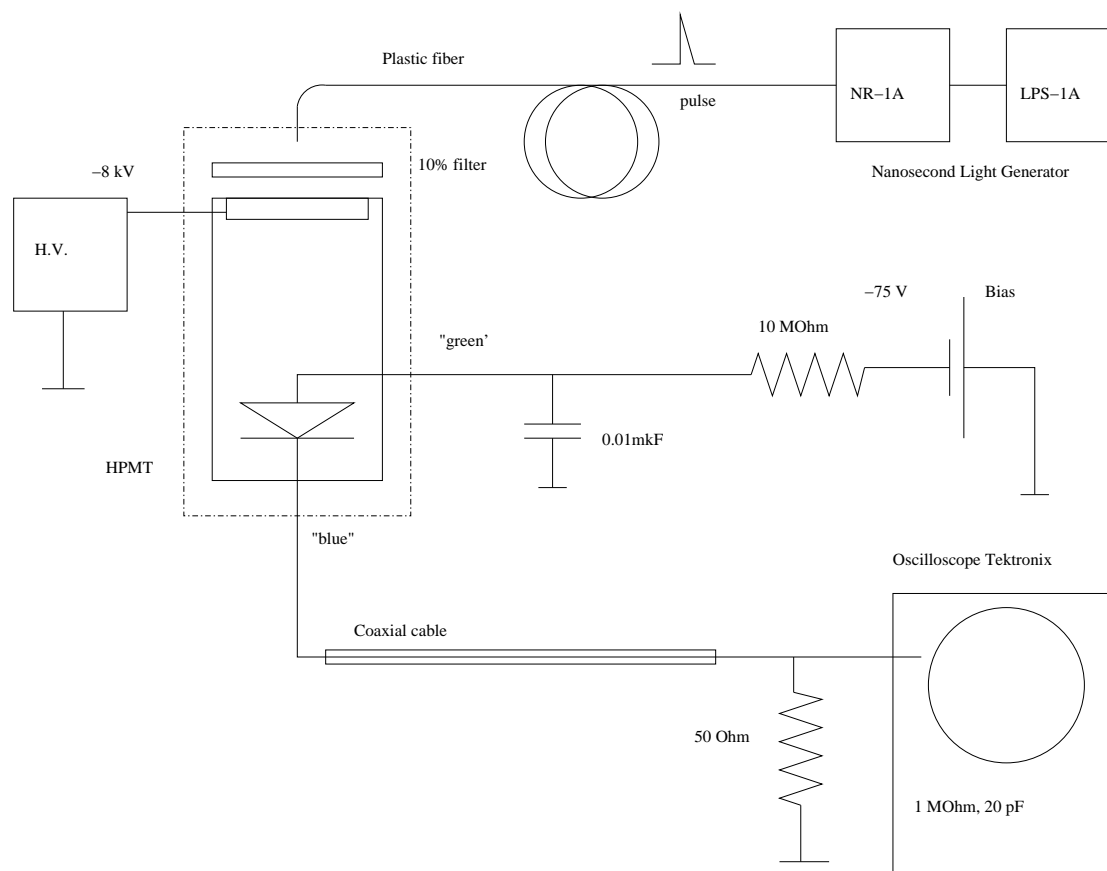


Figure 9: Schematic view of the electronic setup to test the output parameters of a 'barrel' HPD. The structure of HPD is presented inside dashed box. 'Green' and 'blue' correspond of the color of wires coming from the PIN diode. A 10% neutral filter was used to attenuate the light intensity. The Tektronix oscilloscope with input parameters 1 MΩ and 20 pF was used to measure the rise time and the amplitude of signal from the HPD. A Nanosecond Light generator (LPS-1A with NR-1A) was used as a source of light pulses with a duration of a few nanoseconds. Bias - Bias supply for DIN detector of HPD. Dual regulated power supply, model LPD 425FF; H.V. - Power supply PP0100Z (0 to -9 kV). During the tests, the 50 Ω shunting resistance was changed to 100 Ω or completely removed.

Table 2: **Rise time and signal amplitude vs. the capacitance between the HPD and the CREMAT pre-amplifier**

Type of Tube	C[pF]	Rise time[ns]	TRT	Ampl.[V]	Channel	Noise[mV]
HPD	22000	150	141	1.3	950	+/- 3
-/-	10000	150	140	1.4	1100	+/- 3
-/-	200	100	80	0.6	500	+/- 3
-/-	100	55	60	0.4	310	+/- 3
-/-	50	40	43	0.25	210	+/- 3
-/-	25	35	32	0.12	100	+/- 3
PMT	-	<10		8	-	+/- 2

**Notes are itemized below**

- **A:** Signal amplitude measured by Oscilloscope Tektronix 465B (input: 1 M $\Omega$ , 20 pF).
- **Light Source:** Nanosecond Broad-Spectrum Optical Pulse Radiator (Model NR-1A) and Laser Pulse Simulator (Model LPS-1A). High Voltage: 20 kV. Additionally, 10% filter (neutral density) was used.
- **HPD:** A 25 mm proximity focused single pixel Hybrid Photo Diode equipped with an S20UV photo-cathode on a quartz input window. High Voltage: 8 kV, Bias: 75 V. Si Diode capacity: 200 pF.
- **PMT:** Model: BURLE 8575. Used High Voltage: -2 kV.
- **TRT:** Theoretical Rise Time calculated by equation:
 
$$T_{RT} = 2.30 \times Z_{in} \times C_x + T_\rho + T_l,$$
 where:  $T_\rho$  is the pulse rise time with no added input capacitance (13 ns for CR-101D);  $Z_{in}$  is the input impedance (270  $\Omega$  for CR-101D);  $T_l$  is the rise time connected with Light Source and PIN Diode (we used  $T_l=5$  ns);  $C_x$  is the added capacitance. In our case:  $C_x = C_d \times C / (C_d + C)$ ; where  $C_d=200$  pF (HPD Photo Diode capacitance) and C is used capacitance indicated in table.
- **Rise time** was measured between 10% and 90% the height of pulse amplitude.
- **Channel:** Channel number corresponds to the peak position in the spectrum from the light source. An ORTEC 582 shaping amplifier (Gain=10, shaping time 10  $\mu$ s) was used.

### 2.3.2 Spectroscopic Response

In order to measure the ADC (energy) response of the HPD to various ionization sources, the circuit shown in Figure 10 was assembled. Specifically, the energy spectra for  $^{241}\text{Am}$  and  $^{137}\text{Cs}$  were measured using a multi-channel analyser (MCA). These spectra are shown in Figures 11 and 12, and agree with similar measurements in the literature [3, 4].

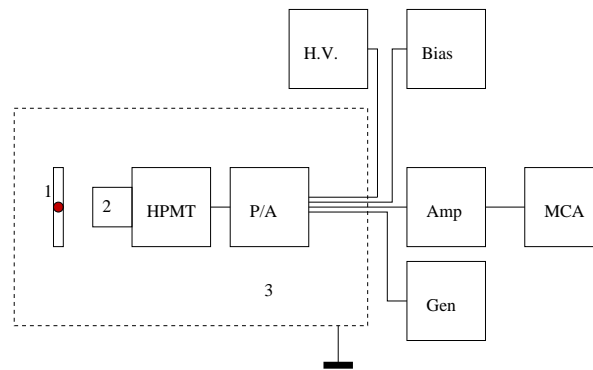


Figure 10: Schematic view of the electronic setup used to test the spectrometric parameters of the HPD. 1 - Source of ionization emission ( $\text{Cs-137}$ ,  $\text{Na-22}$ ,  $\text{Co-60}$  etc.); 2 - Scintillation crystal ( $\text{NaI(Tl)}$  or 'fast' scintillator); 3 - Cylindrical copper box ( $\varnothing 8*17$  cm with 1 mm wall thickness); HPD - Proximity Focused DEP HPD, type PP0350G; P/A - Charge sensitive pre-amplifier, CREMAT CR-101D; Amp - Shaping (spectroscopy) amplifier, ORTEC 572; Gen - Precise pulse generator, ORTEC 419; MCA - Multi-channel pulse-height analyzer, Tektronix 5200; Bias - Bias supply (-80 V) for DIN detector of HPD. Dual regulated power supply, model LPD 425FF; H.V. - Power supply PP0100Z (0 to -9 kV).

Specifically, the  $^{241}\text{Am}$  spectrum clearly shows the 5.5 MeV peak around MCA channel 650, and with a FWHM of approximately 90 channels, which corresponds to an energy resolution of 14%. On the other hand, the  $^{137}\text{Cs}$  spectrum shows the characteristic 662 keV total absorption line (peak around channel 450 in the MCA spectrum) as well as the corresponding Compton distribution.

The energy resolution calculated from the FWHM of the total gamma capture peak

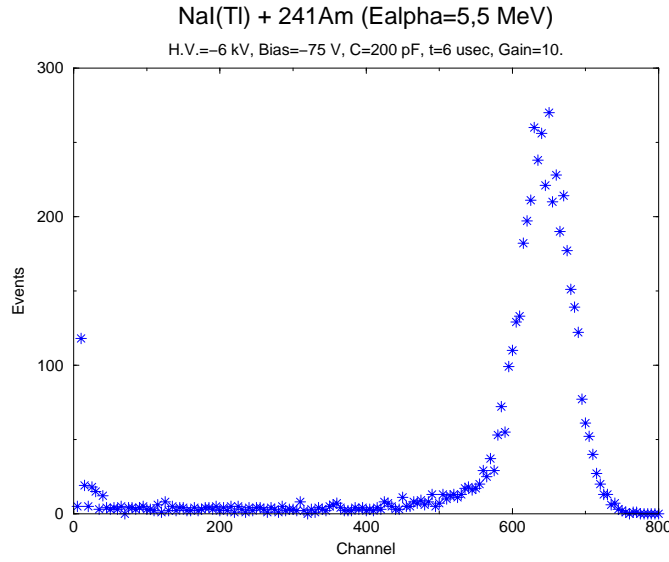


Figure 11: Energy distribution of alpha particles from  $^{241}\text{Am}$  with energy 5.5 MeV as measured with NaI(Tl) scintillator ( $\varnothing 6$  mm and depth of 10 mm). The electronic setup indicated in figure 10 was used. The ionization source was embedded in a scintillation crystal. The operating parameters of a spectrum tract were: High Voltage: -6 kV; Bias voltage: -75 V; Amplifier gain: 10; Shaping time of amplifier: 6  $\mu\text{s}$ .

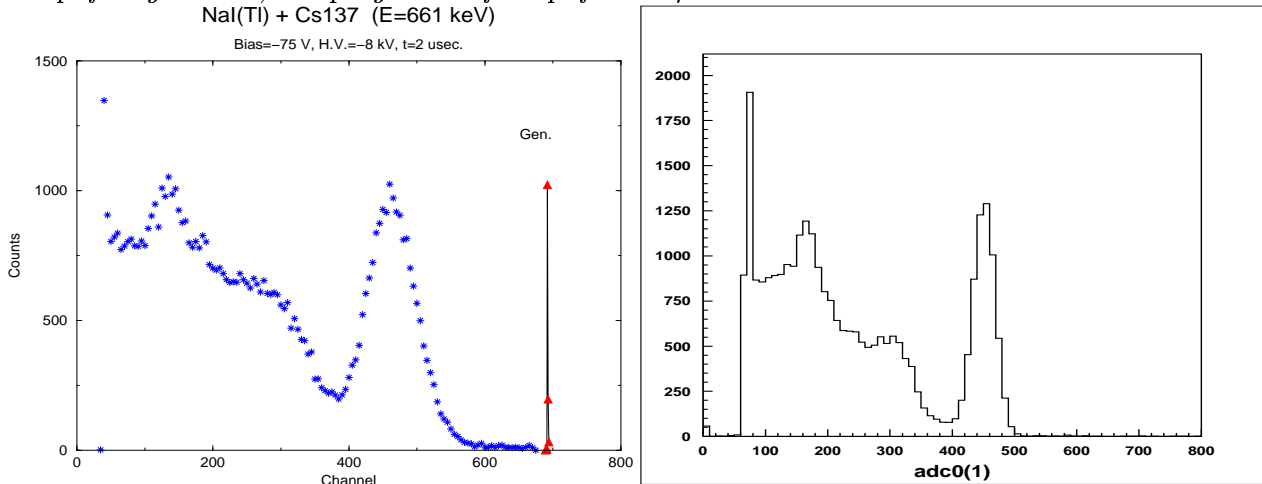


Figure 12: **Left panel:** Energy spectrum distribution of gamma rays from  $^{137}\text{Cs}$  with energy 662 keV as measured with NaI(Tl) scintillator ( $\varnothing 25$  mm and depth of 30 mm) and a MCA. Additionally, the spectrum distribution from the precise pulse generator (ORTEC 419) is shown. The signal from the ORTEC 419 pulse generator was fitted to a test input (pin 3) of the charge sensitive pre-amplifier CR-101D. The energy resolution calculated by the peak of total gamma capture from 662 keV gamma rays was 13.7%. High Voltage: -8 kV; Bias voltage: -75 V; Shaping time of amplifier: 2  $\mu\text{s}$ . **Right panel:** the same spectrum measured via a 2" PMT at  $\approx 1300$  V, a CAMAC ADC and a PC-based data acquisition system.

corresponding to the 662 KeV gamma rays was 13.7%. The same spectrum measured with a standard 2" vacuum PMT connected with a CAMAC ADC and PC-based data acquisition system is shown in Figure 12. The schematic view of the associated electronics set up is presented in Figure 13. In the PMT case, an ADC2249W (W=wide) unit was used instead of the more common ADC2249A unit because NaI(Tl) scintillators have a very long decay time, necessitating an ADC “gate” width of about  $3\mu s$  that can only be handled by a ADC2249W. The resulting energy resolution obtained for the  $^{137}Cs$  gamma source (using the HPD and ADC CAMAC) was 10%. The ADC spectrum obtained with ADC2249W block and  $3\mu s$  gate width has its pedestal at channel 50. The pedestal location increases with the gate width.

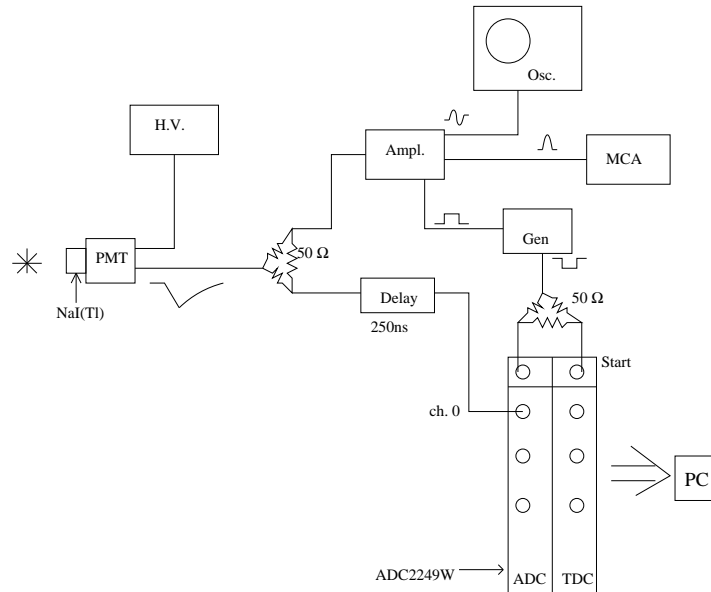


Figure 13: Schematic view of the electronic setup used to measure the spectroscopic response of a 2" PMT (BURLE 8575) to a  $^{137}Cs$  gamma source, using a NaI(Tl) crystal as the scintillator. All elements of the setup are clearly labeled.

### 2.3.3 Amplitude versus Gain

The peak position of the HPD signal was measured as a function of the applied HV on the device. As expected, a completely linear response was extracted, in agreement with the manufacturer's measurements as depicted in Figure 4. The results are plotted in Figure 14.

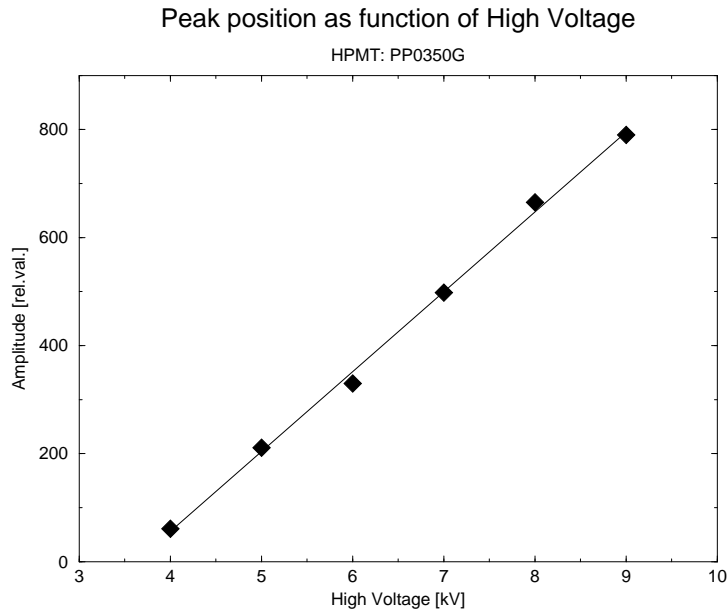


Figure 14: *The amplitude of the signal versus acceleration (photo-cathode) voltage. A  $^{137}\text{Cs}$  source was placed on a NaI(Tl) scintillation crystal. The plotted amplitude corresponds to the MCA channel number of the 662 KeV gamma ray total absorption peak. Bias Voltage: -75 V. The signal was not observed below -3 kV.*

### 2.3.4 Peak Position versus Bias Voltage

Subsequently, the behaviour of the HPD was studied as a function of the applied bias across the PIN diode. The measurements were conducted at two different high voltage values, -6 kV and -8 kV. DEP recommends an operating bias of around 80 V. As observed in Figure 15, the amplitude (peak position) is nearly constant over a broad range of the applied bias.

### 2.3.5 Low light level measurements

DEP claims that their electrostatically focused HPDs can even resolve the single photo-electron peak, as shown in Figure 16. However, no similar information could be obtained from DEP on their proximity focused HPDs, like the PP0350G. Therefore, in order to investigate this issue, the energy spectrum of the PP0350G was measured under low-light conditions, using the setup described in Figure 17.

The results of these measurements pointed to the inability of the PP0350G to resolve the single photo-electron peak. Nevertheless, although the precise amount of light provided to the

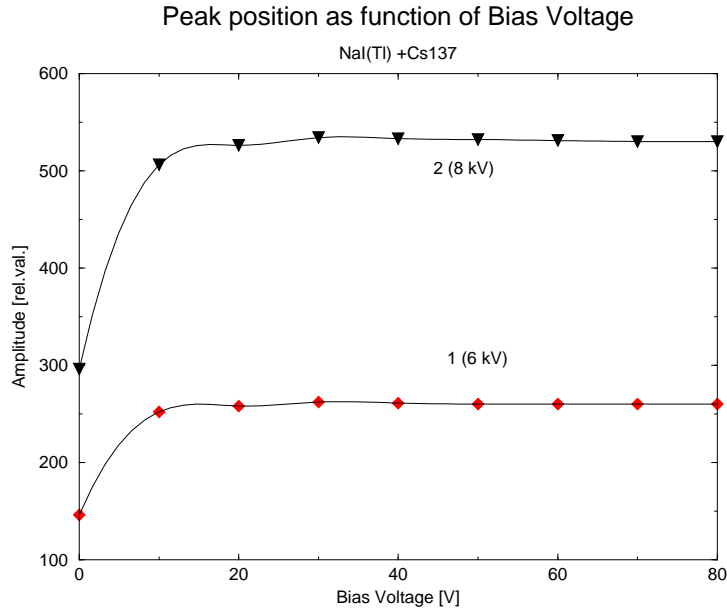


Figure 15: *The amplitude of the signal versus bias voltage of PIN detector. Curves 1 and 2 correspond to -6 kV and -8 kV acceleration (photo-cathode) voltages, respectively. A  $^{137}\text{Cs}$  source was placed on a NaI(Tl) scintillation crystal. The value of 'zero' bias voltage was checked using a standard digital multimeter and the value of 69 mV was observed.*

HPD was not known, based on the shape of the resulting energy spectrum it was surmised that the incident light was equivalent to a few (5-8) photo-electrons. The approximate location of the single photo-electron peak was obtained from the spectral response of the PIN diode in the HPD when irradiated by a  $^{137}\text{Cs}$  gamma source without the application of high voltage.

The MCA spectrum with and without the LED light is portrayed in Figure 18. The left side (no light) shows the pedestal and small noise peaks in the MCA channel, whereas the right side (LED light transported via a clear fiber) shows the same three small peaks on the left (the two curves are not normalized with respect to each other) as well as the several-photo-electron distribution (bump at higher values). Thus, even though the spectrum in Figure 18 does not possess the resolution of the one in Figure 16, in the planned application of the PP0350G as BCAL readout device, single photo-electron capability is not a critical criterion. A quantitative determination of the HPDs energy resolution is still pending.



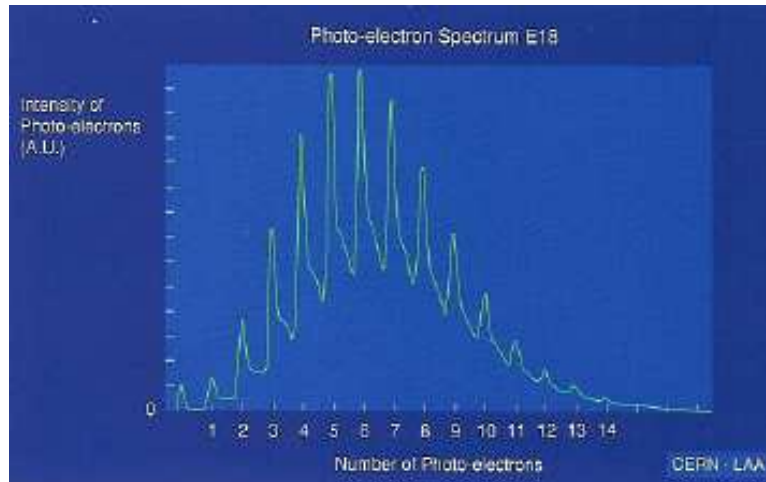


Figure 16: Intensity of photo-electrons for an electrostatically focused HPD (E18).

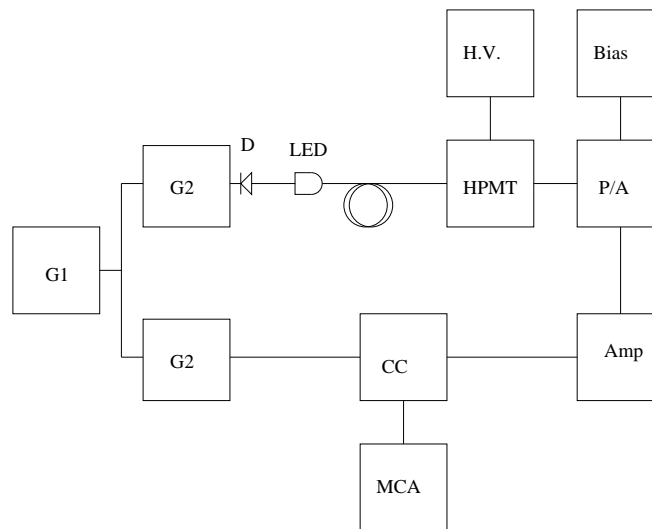


Figure 17: Schematic view of an electronic setup for the spectrum measurement of signals from single photo-electrons. The light from LED transformed by clean plastic fiber was used. G1 - BNC Pulse Generator, model GL-3; G2 - Function Generator 'Krohn-Hite', model 5200A; D - a diode used for LED protection against negative pulses from G2 generator; LED - a source of light; HPD - Proximity Focused DEP HPD, type PP0350G; P/A - Charge sensitive pre amplifier, CREMAT CR-101D; CC - a block of coincidence inside MCA; Amp - Shaping (spectroscopy) amplifier, ORTEC 572; MCA - Multi-channel pulse-height analyzer, Tektronix 5200; Bias - Bias supply (-80 V) for DIN detector of HPD. Dual regulated power supply, model LPD 425FF; H.V. - Power supply PP0100Z (0 to -9 kV).

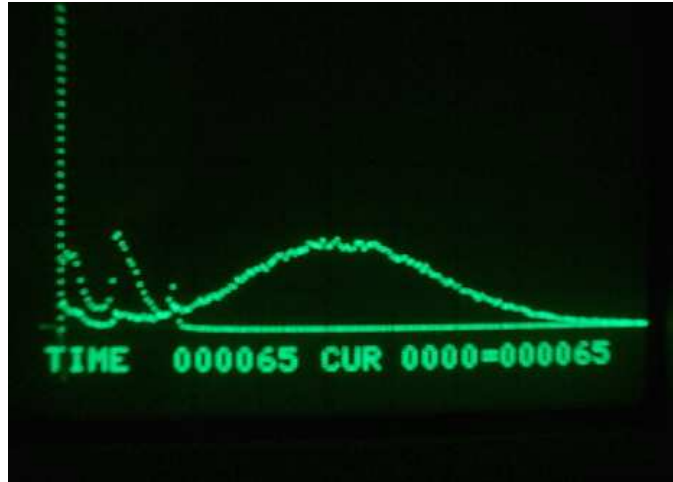


Figure 18: *The spectral response of HPD to a low intensity light source. Unfortunately, the energy resolution of proximity focused HPD from  $\varnothing$ 25 mm silicon PIN detector did not allow for the resolution of the single photo-electron peak. The broad bump in the figure corresponds to several photo-electrons. The electronic setup presented in Figure 17 was used.*

### 2.3.6 Photo-cathode positional sensitivity

The uniformity of response of the PP0350G across the photo-cathode is shown in Figure 4. This attribute is critical for the BCAL readout, for the following reason.

The embedded scintillating fibers in the lead matrix are arranged at a constant pitch between them, within each of the fiber layers. Every pair of adjacent fibers together with the fiber, say, directly in the above layer and positioned along the mid-plane of the pair, form an equilateral triangle with sides measuring 1.35 mm, for the current matrix design which employs  $\varnothing$ 1 mm fibers.

In order to reduce the number of readout channels, two actions are required:

- The readout fibers must be packed closer together than the scintillating fibers which are imbedded in the lead matrix, in order to minimize the “dead” volume where the lead resides. This can be accomplished by using a fiber-to-fiber mask/coupler and then bundling the free end of the readout fibers together. A factor roughly equal to two can be gained from this.
- A further area reduction factor must be applied, by employing a Winston cone that couples to the light guide. A light-mixer pipe will precede the Winston cone, in order

to thoroughly mix the light from the different parts of the BCAL readout section. Typically, a factor of four in area reduction can be achieved by using this technique.

The final optical connection to the HPD will be accomplished using a short, cylindrical disk or light pipe, which will match the area of the photo-cathode. Although the light passing through the mixer no longer has memory of its origin, in the eventuality that the mixer does not operate perfectly, one desires a uniformity of response of the photo-cathode to further suppress any geometrical correspondence of the light. Said otherwise, any non-uniformity in the photo-cathode's response could result in a systematic suppression or enhancement of a particular BCAL region and thus skew the particle identification algorithm and as a result affect the Partial Wave Analysis.

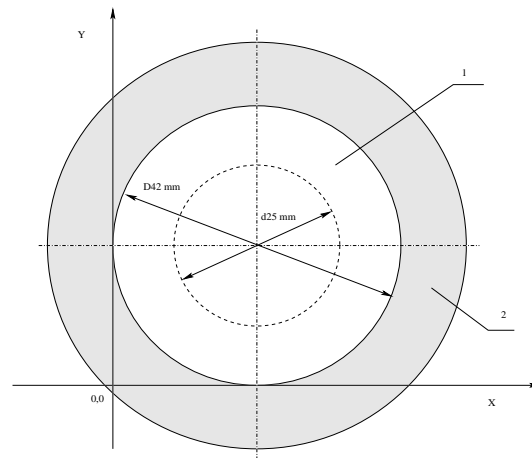


Figure 19: Schematic front view of HPD (Model PP0350G). All dimensions are indicated in mm. The axes (X and Y) indicate the real position of 'x' and 'y' coordinates in measurement of surface sensitivity. 1 - Fused Silica with  $\varnothing 42$  mm. The dashed circle with  $\varnothing 25$  mm corresponds to position of PIN detector inside HPD; 2 - Metallic corpus,  $\varnothing 60$  mm

Therefore, it was important to measure the positional uniformity of the photo-cathode. The photo-cathode and diode are both circular with an active diameter of 25 mm, as shown in Figure 19. This was accomplished by using an LED light source and clear fiber, and scanning the fiber across a two-dimensional grid on the photo-cathode by using the base mount of a standard lab microscope, which allows for a smooth linear translation of the

microscope, or in our case, the clear fiber. The three-dimensional lego plot of the results is shown in the left panel of Figure 20. A clearer view can be obtained by examining a slice of this plot, as displayed in the right panel of Figure 20. From the latter plot it can be seen that the response remains at 90% of maximum out to a diameter of 17 mm, whereas it drops to 50% near the edge ( $\varnothing 25$  mm). This performance is quite acceptable in combination with the light mixer.

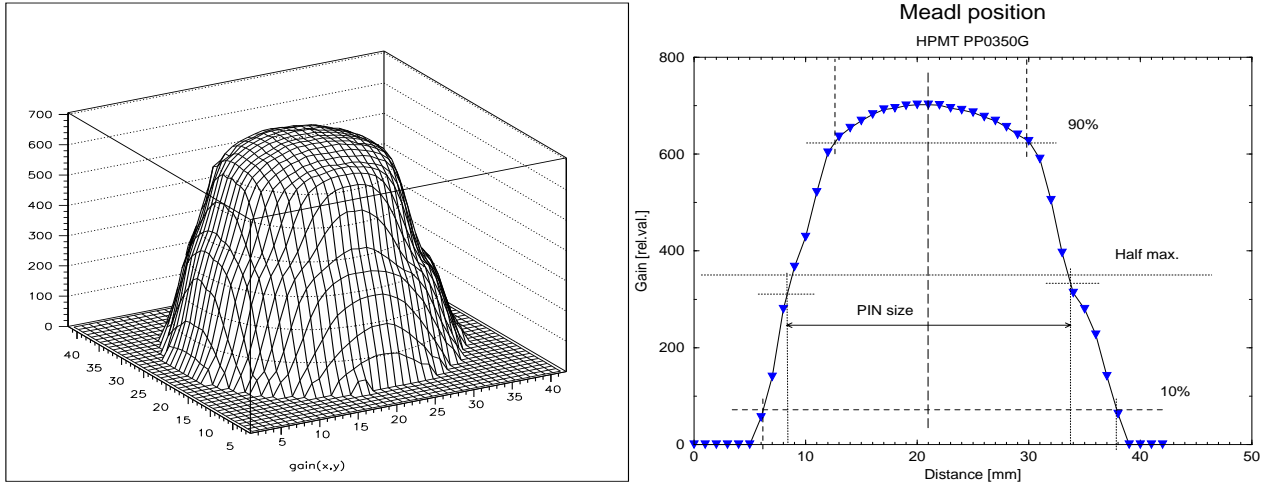


Figure 20: **Left panel:** The lego plot of relative gains at different points on the surface of the fused silica of the PP0350G. The size across the 'x' and 'y' directions is indicated in 'mm'. The point with coordinate (0,0) corresponds to coordinate (0,0) in Figure 19. The light source from the LED was transported using a clear fiber. In measurement, the HPD was mounted on special assembly and the plastic fiber was scanned across the surface of HPD in 1 mm steps. The distance between the edge of fiber and the surface of HPD was less than 0.5 mm (and the fiber never touched the fused silica's surface). The fiber was scanned perpendicular to the surface of HPD. High voltage: -8 kV. Bias voltage: -75 V. **Right panel:** Relative gain at different points along a center line of sensitive surface of HPD (the cross section of Figure 20 across surface with  $y=21$  mm coordinate). The diameter where the gain decreased to 90% from maximal value was 17 mm. At the distance of 12.5 mm from center of the sensitive surface, corresponding to the size of PIN diode, the value of gain decreased by more than a factor of two.

### 3 Summary and Conclusions

During the period between September 2001 and May 2002, a PP0350G HPD from DEP was tested in a number of different configurations and using various connection circuits whose key component was a CREMAT CR-101D pre-amplifier.

The key studies involved: a) the study of rise time and amplitude of HPD signals, b) the investigation of the spectroscopic response (energy spectrum), c) the measurement of the amplitude vs. gain relationship, d) the examination of the ADC Peak position as a function of diode bias voltage, e) the attempt to measure low light levels (few photo-electrons), and f) the verification of the manufacturer's photo-cathode positional sensitivity.

Several additional investigations are being planned. These will involve a further optimization of the pre-amp choice and circuit, further RF noise and ground loops studies, and, finally, tests in a high magnetic field at IUCF. To this point, however, there appear to be no show-stoppers in the selection of the DEP PP00350G as the readout device of choice for the GlueX Barrel Calorimeter.

## References

- [1] A.R. Dzierba, C. A. Meyer, E. S. Swanson, *The Search for QCD Exotics*, American Scientist, (2000) 406–415.
- [2] A.R. Dzierba, N. Isgur, *Mapping Quark Confinement by Exotic Particles*, CERN Courier, (1999).
- [3] C. D'Ambrosio *et al.*, NIM A **431** (1999) 455.
- [4] C.P. Datema *et al.*, DEP Internal Report.
- [5] Pol.Hi.Tech. s.r.l.0, Carsoli, Italy.
- [6] Dow Corning Corporation, Part No. Qw-3067, Midland, Mich., 48640, U.S.A.
- [7] L. Snook, *Hybrid Photo-multiplier Tubes for Hall D/Jefferson Lab*, SPARRO Group Internal Report, August 2001.
- [8] The TRIUMF MIDAS Data Acquisition system, <http://midas.triumf.ca/>
- [9] S. Vidaković, *Tests of Scintillating Fibers for the Hall D Barrel Calorimeter*, SPARRO Group Internal Report, August 2001.
- [10] BICRON Corporation, Newbury, Ohio, USA.